PCH PhysicoChemical Hydrodynamics Vol. 11, No. 1, pp. 103–112, 1989.
Printed in Great Britain

0191–9059/89 $3.00 + .00
Pergamon Press plc

SURFACE TENSION MEASUREMENTS BY THE OSCILLATING DROPLET METHOD

W. J. HILLER and T. A. KOWALEWSKI

Max-Planck-Institut für Strömungsforschung, 3400 Göttingen, F.R.G.

(*Received 16 June 1988 and in revised form 8 August 1988*)

Abstract—An optical method for the measurement of instantaneous values of surface tension has been developed. This method depends upon the relationship of the frequency of an oscillating liquid droplet to the surface tension of the fluid. The droplets used have radii of approx. 0.15 mm and are obtained by the break up of a liquid jet. Experiments were performed with water and ethanol. The results are in reasonable agreement with values obtained by the static ring method.

1. INTRODUCTION

For most processes involving liquids with free surfaces, interfacial tension plays an important role. Such processes include the disintegration of liquid jets, the generation of bubbles or formation of emulsions, as well as Marangoni-type flows and the evaporation from liquid surfaces. As surface tension depends not only on temperature but in many cases is also very sensitive to impurities dissolved in the medium, one often needs to know its instantaneous value. The aim of the present paper is to report on the first non-intrusive surface tension measurements, by which the motion of oscillating droplets is analyzed with the help of a high speed imaging device.

2. DROPLET OSCILLATIONS

In the absence of external forces, an initially distorted liquid droplet finally reaches an equilibrium spherical shape. This process is generally accompanied by a series of damped oscillations. A particular oscillatory mode is completely described by the oscillation frequency and the amplitude decay rate (as long as the oscillating system behaves linearly). The oscillation frequency and the damping depend on the surface tension, the density and viscosity of the fluid and the radius of the droplet. There are several more or less complicated theoretical models describing this phenomenon. The question arises as to what are the limiting experimental conditions for which the theoretical model will be applicable and oscillation analyses will provide sufficiently accurate surface tension results.

An appropriate mathematical analysis of oscillating droplets when both fluids are inviscid may be found in Lamb's "Hydrodynamics" (1932). For small amplitude oscillations he obtained the following simple formula for the frequency of the nth mode of oscillation:

$$\Omega_n^2 = \frac{(n-1)\cdot(n+1)\cdot(n+2)\cdot n\cdot\sigma}{[(n+1)\cdot\rho_i+n\cdot\rho_e]\cdot R^3}, \tag{1}$$

where σ is the interfacial tension between the two phases, ρ_i and ρ_e are the densities of the internal (droplet) and external phase, respectively, and R is the radius of the droplet at equilibrium. As $n = 0$ and $n = 1$ describe no oscillations at all, the first mode of interest is $n = 2$ (which corresponds to the oscillation of a spheroid). For $n = 2$ and in the case that the density ρ_e of the surrounding medium is negligible compared with the density of the droplet medium, one obtains:

$$\Omega^2_{\mathrm{Lamb}} = \frac{8 \cdot \sigma}{\rho_i \cdot R^3}. \tag{2}$$

The analysis of droplet oscillations was extended to include viscosity effects by Chandrasekhar (1959, 1961), Reid (1960) and Valentine *et al.* (1965). The general solution for a viscous droplet oscillating in a viscous fluid was given by Miller & Scriven (1968) and Prosperetti (1980a,b). From these calculations it follows that for sufficiently large droplets of a low viscosity fluid, for example water droplets with diameters larger than 10 μm oscillating in a gas, the oscillation frequency deviates less than 1% from that one given by equation (2). However, as a consequence of the liquid's viscosity, the oscillations are damped so that the amplitude A_n of the nth mode will decrease exponentially according to:

$$A_n = A_{n0} \exp(-t/\tau_n), \tag{3}$$

where A_{n0} is the amplitude at the time $t = 0$ and τ_n the decay factor of the nth mode.

Generally, the amplitude decay factor τ_n, calculated by Prosperetti (1980a) for viscous droplets oscillating in another viscous medium, is a complicated function of the oscillation frequency, Ω, and of the densities and viscosities of the external and internal fluids. For viscous droplets dispersed in a vacuum or gas, however, Prosperetti's result simplifies to the following relation:

$$\tau_n = \frac{R^2}{\nu(n-1) \cdot (2n+1)}, \tag{4}$$

where ν is the kinematic viscosity.

It follows, for example, that for water droplets of 0.1 mm radius the decay factor of the second mode is $\tau_2 = 2 \cdot 10^{-3}$ s and for the third mode $\tau_3 = 7.1 \cdot 10^{-4}$ s. The third mode is damped almost three times faster than the second one. This means that during a few periods at the end of an oscillatory motion, a droplet will generally oscillate in the second mode which, due to its spheroidal shape, can be easily analyzed. Three characteristic features of droplets oscillating in the 2nd mode in air, are displayed as a function of droplet radius for three different liquids in Figs 1–3. These are: the oscillation frequency Ω_L described by equation (2); the normalized deviation, $\delta = 1 - \Omega/\Omega_L$, of the Lamb's oscillation frequency, Ω_L, from the more accurate values of Ω as given by Prosperetti (1980a) and Brosa (1988a), respectively; and the number of oscillations, N, during which the amplitude decreases to $1/e$ (≈ 0.37). The results of Prosperetti displayed in Figs 1–3 are drawn with help of his asymptotic expression for a viscous droplet in a viscous medium (1980a, equation 54). In this paper he defines a dimensionless viscosity, $\varepsilon = \nu \cdot (\rho/R \cdot \sigma)^{1/2}$, values of which we also put on the abscissa. According to his calculations, the viscous correction to the oscillation frequency, Ω_L, of the droplet is negligibly small if $\varepsilon < 0.1$ (compare with Figs 1–3). Brosa (1988a) proposed a straightforward numerical solution of the equation of motion for a viscous globe oscillating in a vacuum (a problem which was discussed earlier by Chandrasekhar, 1959 and Reid, 1960). Figures 1–3 show that for droplets with radii $R > 0.1$ mm, as we intend to use them in the experiment, this model gives deviations, δ, from Lamb's frequency well below 1%.

The dependence of N on the droplet radius (Figs 1–3) indicates the limits of the observation method proposed. For a droplet where the amplitude decreases very fast

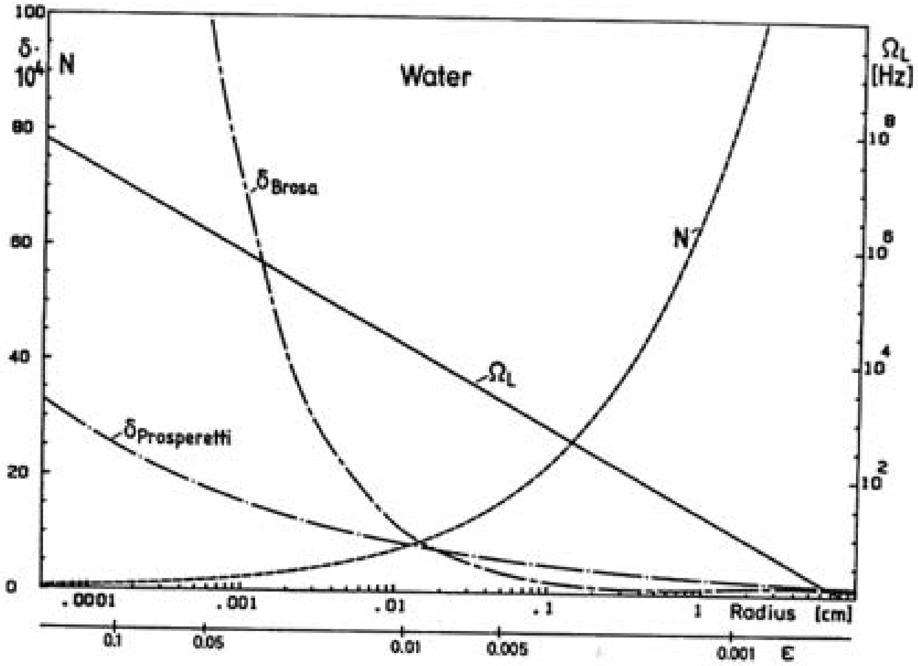

Figs. 1–3. The second mode oscillation frequency, Ω_L; the normalized deviation, $\delta = 1 - \Omega/\Omega_L$, of the Lamb's frequency, Ω_L, from the "viscous" frequency, Ω, given by Brosa and Prosperetti; and the number, N, of oscillations during which the amplitude of the 2nd mode decays to 1/e—shown as a function of the droplet Radius, R, and of the dimensionless parameter ε. This figure shows water.

($N \leqslant 1$), observation and evaluation of the oscillation frequency will become more complicated than for high values of N. Very small droplets are expected to perform no oscillations at all, as in this case an excited droplet will return aperiodically to its spherical shape. A detailed study of these questions has been performed by Chandrasekhar (1961)

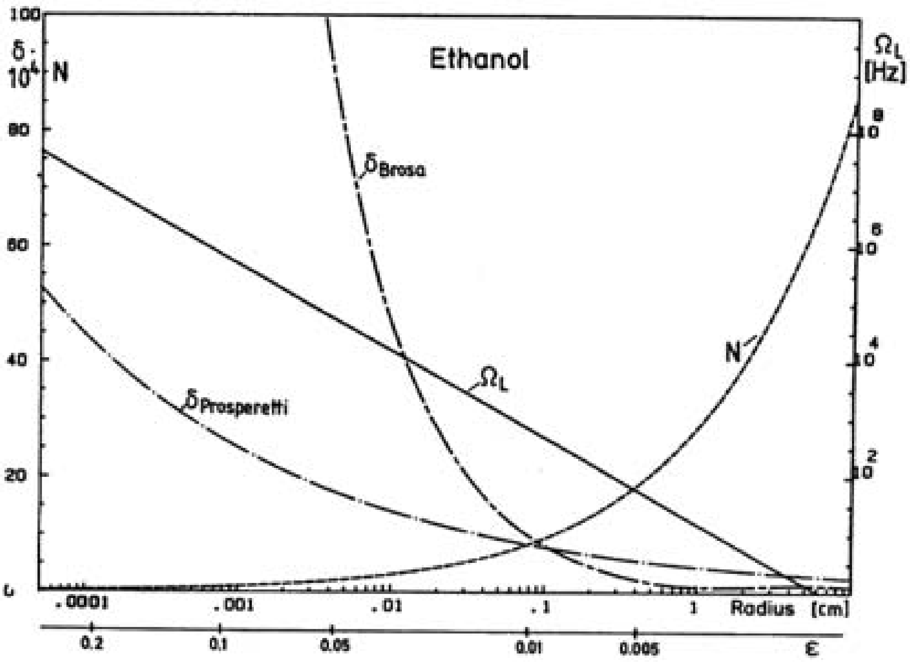

Fig. 2. As Fig. 1, but for ethanol.

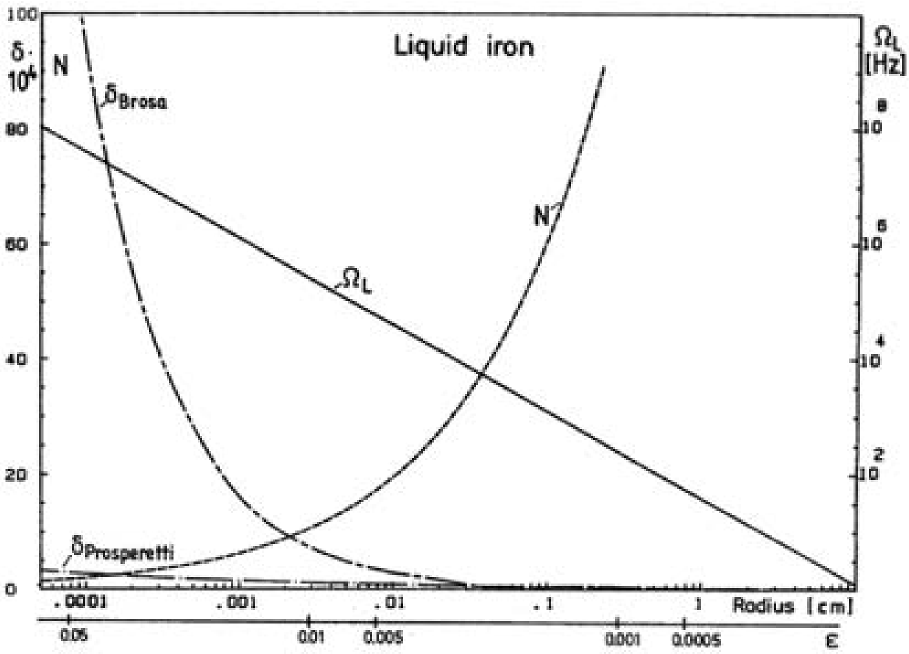

Fig. 3. As Fig. 1, but for liquid iron.

and Reid (1960), who found that the critical radius for a water droplet below which this aperiodic decay occurs is equal to $2.3 \cdot 10^{-6}$ cm.

Up to now, we have discussed only linear oscillations. Recently, Brosa (1988b) communicated some first results on non-linear oscillations for the case of a non-viscous spheroidal droplet. From his model we get a rough upper estimate for the maximum frequency decrease for large amplitude oscillations. It follows that for a normalized oscillation amplitude $A/R \approx 25\%$ the frequency decrease is less than 5%. This means, then, that the influence of the non-linearity on the measuring accuracy can be kept negligibly small, provided the amplitudes are not too large. On the other hand, however, for large amplitude oscillations non-linear effects, as described by Becker (1988), will become a dominating feature in drop dynamics.

It should be mentioned that Prosperetti (1980b) has also obtained a solution to the initial value problem giving theoretical predictions concerning the behaviour of oscillating droplets in the early transient period. His remarks on the time dependence of both the damping factor, τ, and the oscillation frequency, Ω, are very important for studies of the initial oscillation behaviour of the droplet. However, asymptotic values of Ω and τ, which he obtains for large time, are equal those given by normal mode analysis. In other words, the final cycles of droplet oscillations can be correctly described in terms of a periodic oscillator motion.

From above considerations it can be concluded that the oscillation in air of low viscous droplets of diameter larger than 10 μm will be sufficiently accurately described by the simple formula of Lamb (2), provided we limit our study to the last periods before the oscillations cease.

3. EXPERIMENTAL

An overall view of the experimental set-up is displayed in Fig. 4. It consists essentially of three devices: a drop generator; a high speed stroboscopic light source and imaging

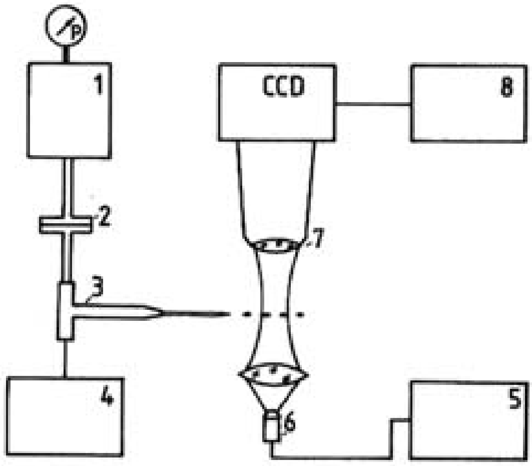

Fig. 4. Experimental set-up. (1) pressurized reservoir; (2) teflon filter; (3) drop generator; (4) piezo-driver; (5) LED pulse driver; (6) LED; (7) microscope with CCD camera; (8) image processor and computer.

unit; an image processor connected to a computer. The droplets are generated by the break-up of a laminar liquid jet. The liquid, supplied through teflon tubes and a teflon filter from a pressurized tank, is discharged from a nozzle with a 0.1 mm diameter orifice. To reduce contamination of the fluid all parts of the nozzle that may come into contact with the liquid are made of stainless steel or copper. In order to control the disintegration process of the jet, artificial pressure disturbances are superimposed on the liquid in the antechamber of the nozzle using a piezoceramic transducer (Fig. 5). By properly adjusting the oscillation frequency of the piezoceramic driver to the eigenfrequency of the jet (the frequency of the capillary instability) the jet can be caused to break up into a row of practically monodispersed droplets. Due to the break up process, the droplets oscillate first in many modes and at large amplitudes. After a short time the second mode, which has the largest decay time, becomes totally dominant. Finally, after a few oscillations (see Figs 1–3), the droplets return to their static form. If the jet separates symmetrically from the nozzle and there are no external disturbances, the oscillating droplets preserve their symmetry axis parallel to the nozzle axis. Aerodynamic forces acting on the droplets moving in a gas or vapour may cause additional shape deformation. In our experiments, however, the droplets move at low velocities between 1 and 2 m s^{-1} and have typical radii of 150 μm so that their final

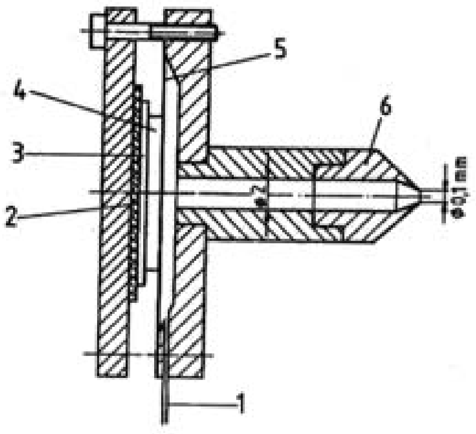

Fig. 5. Scheme of the droplet generator. (1) flow inlet; (2) insulator; (3) electrode; (4) piezo-ceramic disk; (5) stainless steel membrane; (6) nozzle.

shape—within our measuring accuracy of $\approx 0.5\%$—is spherical. This is due to the additional internal pressure, generated by surface tension, which is much higher than the external force variation acting on the droplet.

The oscillations of the droplets are observed through a microscope in bright field illumination, i.e. the projections of the droplets appear as dark objects in the plane of observation. It is therefore important that the axis of symmetry of the droplet lies within the plane of observation. A pulsed Light Emitting Diode (LED), driven by a specially designed pulse generator (Hiller *et al.*, 1987), was used to illuminate the droplets. It allows light pulses to be generated with a repetition frequency up to 2 MHz and pulse widths ranging from 0.05 up to 10 μs. For a droplet velocity of 2 m s^{-1} and a 10-fold magnification of the objective of the microscope, the maximum exposure time, based on the spatial resolution of the camera used in our experiments, was limited to 1 μs. The typical pulse width applied was between 100 and 300 ns. A frame transfer charge coupled device (CCD) was used as a camera. A particle crossing the field of view will be imaged typically 15–20 times onto the sensor region of the CCD camera. The strobe illumination frequency was generally chosen to be between 10 and 30 kHz. In most cases the multiple exposures were taken during the integration time of the frame transfer sensor. The final frame, containing a series of superimposed droplet images which cover, typically, one period of the oscillation, may then be either directly printed on a video printer or stored (via an image processor) in a computer. For simple objects such as the projections of droplets, one can easily extract the shape of boundaries by computer aided image analysis. Using a special numerical fitting procedure, ellipses are then matched to each of these boundaries. The droplet oscillation frequency is evaluated by matching the lengths C of the principal axis of the previously evaluated ellipses to the following function:

$$C(t) = R + A \cdot \sin(\Omega \cdot t + \phi), \tag{6}$$

where A is the oscillation amplitude, which for the present evaluation, is assumed to be constant, Ω the angular oscillation frequency and ϕ the phase angle.

A detailed description of this procedure has been given by Hiller & Kowalewski (1988). If the axis of the oscillating spheroid coincides with the plane of observation, the volume of the droplet calculated from its projection should be constant. This fact is used for controlling and selecting proper image sequences.

Figures 6 and 7 show example photos of the droplets taken by our high speed imaging device. In Fig. 6 a series of 5 successive exposure at interval times of 86 μs is displayed. At the moment when a new drop separates from the jet, its oscillation is generally made of many modes. This is illustrated by the pronounced asymmetry of its shape with respect to the flow direction and by the strong curvature of its boundary. The white spots inside the contours of the droplets and the jet are images of the illuminating light source, as the liquid used is transparent. Due to surface curvature, the jet and the droplets act like a collecting lens. The shape of these spots depends on the local surface curvature and can give information about the spatial form and symmetry of the droplets. If, for example, the white spot is elongated into a straight line, the object has a cylindrical form. This is as one would expect for the undisturbed jet immediately after leaving the nozzle. The successive exposures on Fig. 6 were taken during the frame transfer process of the CCD camera. Such an application of the camera is possible when one is interested in following the behaviour of the jet in time and space. Figure 7 shows an example of a multiple exposure during the integration time of the sensor. Due to the multiple exposure the dynamic range of the photo is low and therefore it is not very impressive to the eye. Computer aided image processing, however, provides sufficient distinctions between small grey level steps so that the shape of

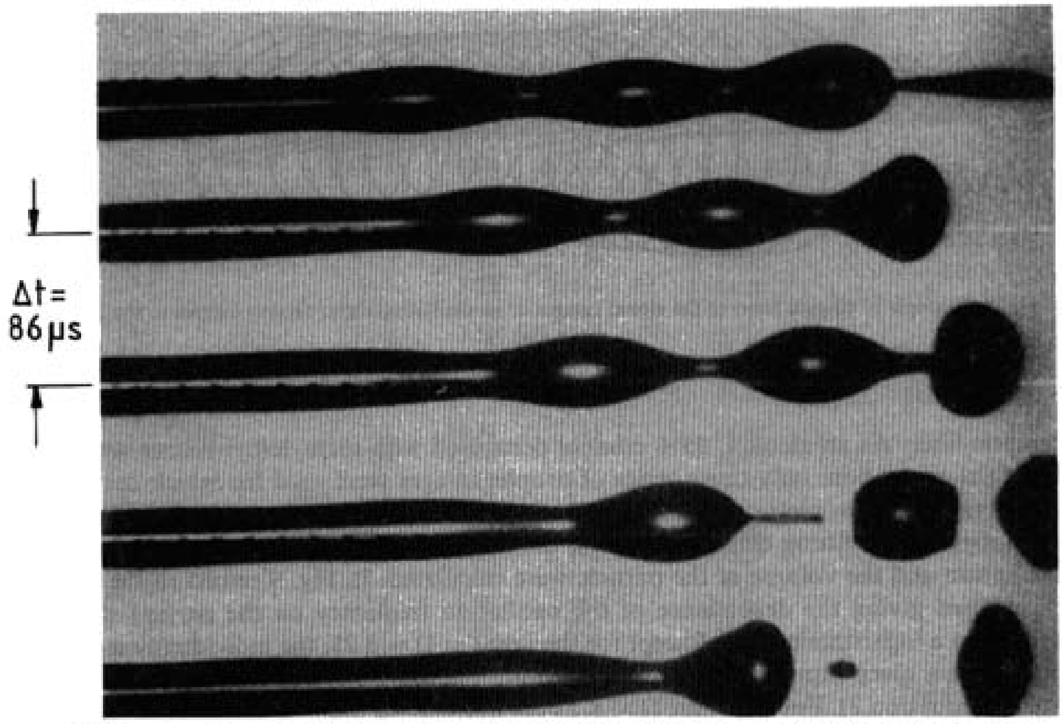

Fig. 6. Break-up of a water jet. Time interval between subsequent images = 86 μs, exposure time = 200 ns, nozzle diameter = 0.1 mm, exciting frequency of the piezo-driver = 3.6 kHz. Picture taken during the frame transfer process.

a single droplet may be evaluated. Figure 8 shows as an example a sequence of 14 ellipses evaluated from such a series of superimposed images.

4. RESULTS

Experiments have been performed with water and ethyl alcohol droplets in air at atmospheric conditions. The water used was filtered tap water cleaned for a second time in an

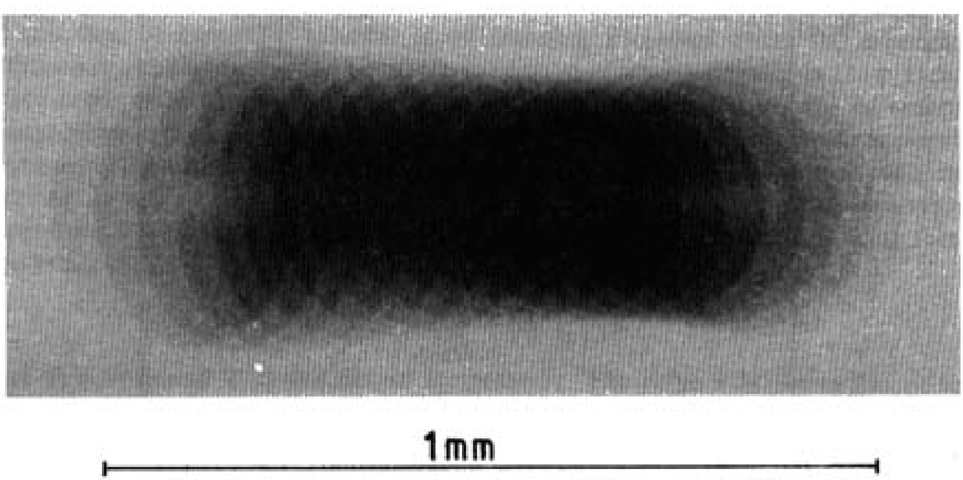

Fig. 7. Multiple exposure of an oscillating droplet during the integration period of the CCD sensor. Strobe frequency 30 kHz.

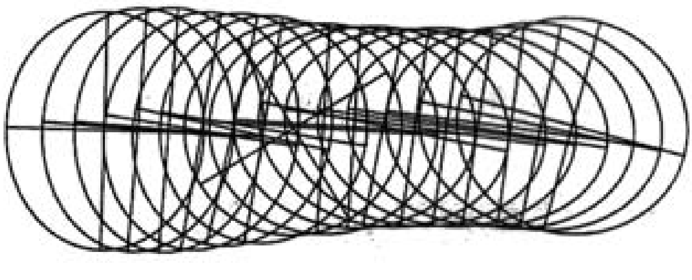

Fig. 8. Example of ellipses fitted to the stored images of an oscillating water droplet (relates to the droplet on Fig. 7).

osmotic filter. As an alcohol, 95% ethanol denatured with methylethyl-ketone was used. For final evaluation, only those series of droplet images were used for which the axis of symmetry of the droplets undoubtedly coincided with the plane of observation. From the axes of the "best fitting ellipses" (Fig. 8), the angular frequency, Ω, of the 2nd mode of oscillation and the volume of the particle were calculated. In Fig. 9 results of the present experiment giving the dependence of the oscillation frequency on the particle radii are shown on a logarithmic scale. Except for the point at $\Omega = 8.25$, the individually measured points for a given liquid can be connected quite well by a straight line as expected from theory (equation 2). For the value $\Omega = 8.25$ the normalized oscillation amplitude A/R was about 32%, giving rise to an apparent frequency off-set. Table 1 summarizes the values of the measured data pairs, together with the calculated values of surface tension. For comparison, the surface tension of both liquids used was measured by the standard ring method. The relative error of a single optical surface tension measurement is 5% when compared to the ring method value. The deviation of the mean value is well below 0.5%, however. Probably due to the fact that the water used was processed by filtering, its surface tension is about $3 \cdot 10^{-3}$ N m^{-1} lower than the standard value for pure water. This indicates how sensitively the surface tension can depend on impurities.

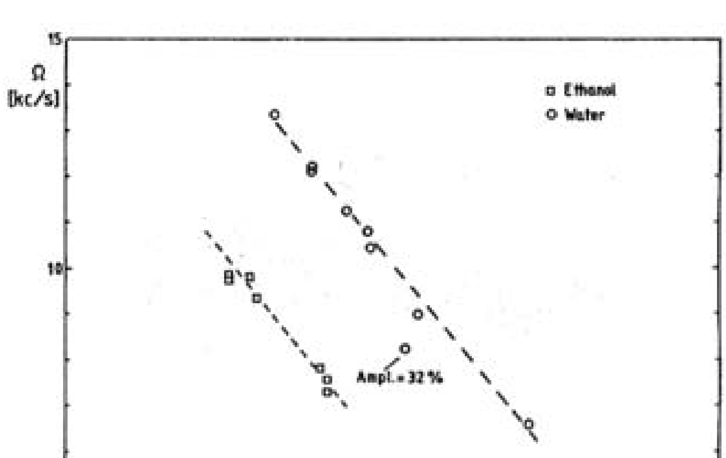

Fig. 9. Measured oscillation frequency as a function of droplet radius.

Table 1. Examples of measured values of surface tension

No.	Liquid	Rel. ampl. A/R [%]	Osc. freq. Ω [kHz]	Droplet radius R [μm]	Calc. σ $\cdot 10^{-3}$ [N m^{-1}]	Measured by ring method σ $\cdot 10^{-3}$ [N m^{-1}]
1	Ethanol	11.1	9.84	134	22.76	
2		11.7	9.77	134	22.45	
3		11.6	9.82	139	25.35	
4		14.0	9.33	141	24.20	
5		14.6	7.80	158	23.55	
6		21.2	7.55	160	23.10	
7		20.2	7.29	160	21.35	
	Mean value				23.25	23.3
1	Water	2.3	13.34	145	68.53	
2		13.0	12.10	155	68.65	
3		7.5	12.19	155	69.82	
4		15.9	11.24	165	71.07	
5		17.5	10.80	171	72.90	
6		15.3	10.45	172	70.19	
7		15.8	10.57	172	70.95	
8		11.8	8.99	187	65.80	
9		7.2	6.60	229	65.07	
10		31.7	8.25	183	52.24*	
	Mean value				69.19	69.3

*This value, obtained for a large amplitude of oscillations, was not taken into account when calculating the mean value.

5. CONCLUSION

Our results indicate that the oscillating droplet method can be developed into a powerful tool for surface tension measurements. As it is a non-intrusive method it can be applied at extreme temperatures, e.g. during spray formation for liquid metals or on subcooled or superheated liquid droplets. Compared with static methods it gives instantaneous values and can thus be especially valuable in all transient processes where the experimental conditions are changing rapidly, i.e. in the formation of jets or droplets in the presence of surface active substances or during the heating and cooling of surfaces. Alternatively, as surface tension depends strongly on temperature, the method may offer the unique possibility of measuring the surface temperature of droplets undergoing condensation or evaporation processes. In such an application one would use the variation of surface tension with temperature T which can be described for most liquids simply by the following formula (Reid *et al.*, 1977):

$$\sigma \approx (1-T_r)^{4n}, \tag{7}$$

where $T_r = T/T_c$ and T_c is the critical temperature. The value n of the exponent varies between 0.25 and 0.31. The dependence of σ on temperature is therefore nearly linear, with a slope in the range of order of $0.15\cdot 10^{-3}$ N m^{-1} K^{-1}. A proper calibration of $\sigma(T)$ for stationary conditions can also be obtained by the ring method. Then measuring the instantaneous values of surface tension of an oscillating droplet, one can calculate from the reciprocal relation $T(\sigma)$ its surface temperature.

REFERENCES

Becker, E. (1988) Asymmetriefluktuationen beim Zerreissen eines Tröpfchens. Diplomarbeit, Universität Marburg.

Brosa, U. (1988a) Strongly dissipative modes. Unpublished, Universität Marburg.

Brosa, U. (1988b) Private communication. Universität Marburg.

Chandrasekhar, S. (1959) The oscillations of a viscous liquid globe. *Proc. London Math. Soc.* **9**, 141.

Chandrasekhar, S. (1961) *Hydrodynamic and Hydromagnetic Stability*, pp. 466–477. Clarendon Press, Oxford.

Hiller, W., Lent, H.-M., Meier, G. E. A. & Stasicki, B. (1987) A pulsed light generator for high speed photography. *Exp. Fluids* **5**, 141.

Hiller, W. J. & Kowalewski, T. A. (1988) An optical method for surface tension measurements of dispersed liquid droplets. In *Proceedings of the ICALEO*, San Diego 1987, Vol. 63 (Edited by W. H. Stevenson), pp. 106–110. Laser Inst. of America.

Lamb, H. (1932) *Hydrodynamics*, 6th edn, pp. 473–475. Cambridge University Press, Cambridge.

Miller, C. A. & Scriven, L. E. (1968) The oscillation of a fluid droplet immersed in another fluid, *J. Fluid Mech.* **32**, 417.

Prosperetti, A. (1980a) Normal-mode analysis for the oscillations of a viscous liquid drop immersed in another liquid. *J. Mech.* **19**, 149.

Prosperetti, A. (1980b) Free oscillations of drops and bubbles: the initial-value problem. *J. Fluid Mech.* **100**, 333.

Reid, W. H. (1960) The oscillations of a viscous liquid drop. *Quart. Appl. Math.* **18**, 86.

Reid, R. C., Prausnitz, J. M. & Sherwood, T. K. (1977) *The Properties of Gases and Liquids*, 3rd edn, p. 612. McGraw-Hill.

Valentine, R. S., Sather, N. F. & Heideger, W. J. (1965) The motion of drops in viscous media. *Chem. Engng. Sci.* **20**, 719.